

DOI: <https://doi.org/10.24425/amm.2023.146232>RUOXU WANG<sup>1,2,3</sup>, LUBEI LIU<sup>1,2</sup>, ZONGHENG XUE<sup>1,2</sup>, TENG TAN<sup>1,2\*</sup>

## INVESTIGATION OF THE MICROSTRUCTURE AND MECHANICAL PROPERTIES OF BRAZING JOINTS BETWEEN NIOBIUM AND 316L STAINLESS STEEL USING SILVER-COPPER-PALLADIUM FILLER

This paper introduces an approach for vacuum brazing of niobium-316L stainless steel transition joints for application in superconducting radiofrequency cavity helium jackets. The study takes advantage of good wettability of Ag-Cu-Pd brazing alloy to suppress brittle Fe-Nb intermetallic formation, hence improve the joints' mechanical performance. The wettability of Ag-Cu-Pd filler metal on niobium, the interface microstructure and mechanical properties of the transition joints were investigated. Two kinds of Ag-Cu-Pd filler metals had been studied and wet well on the niobium, and the wettability of Ag-31.5Cu-10Pd filler metal on niobium was better than Ag-28Cu-20Pd filler metal. Microstructure characterization demonstrated the absence of brittle intermetallic layers in all of the joint interfaces. Mechanical properties of samples prepared with Ag-31.5Cu-10Pd filler metal were also better than their peers made with Ag-28Cu-20Pd filler metal both room temperature (300 K) and liquid nitrogen temperature (77 K). The transition joints displayed shear strengths of 356-375 MPa at 300 K and 440-457 MPa at 77 K, respectively. After undergoing ten thermal cycles between the room temperature and the liquid nitrogen temperature, the transition joints' leak rates were all lower than  $1.1 \times 10^{-11}$  mbar · L/s. Therefore, Ag-Cu-Pd filler metal is applicable to high vacuum vessels used at cryogenic temperatures.

*Keywords:* Ag-Cu-Pd brazing alloy; niobium; vacuum brazing; 316L stainless steel; SRF cavities

### 1. Introduction

Institute of Modern Physics, Chinese Academy of Science (IMP, CAS) is developing an extensive research program on superconducting radio-frequency (SRF) cavity technology to fulfill the need of the Chinese initiative Accelerator Driven Subcritical System (CiADS) [1-3]. These cavities are made of ultra-pure niobium (residual resistivity ratio, RRR, > 250). Therefore, during their operation, liquid helium with temperature of 2K or 4K flows through the space between helium jackets and cavities to cool the SRF cavities, and keeps the niobium material in superconducting state [4]. At present, titanium is chosen as the helium jackets because its thermal expansion coefficient is close to that of niobium [5]. Nevertheless, titanium has the disadvantages of manufacturing difficulties and high costs. Therefore, many laboratories have been investigating alternative material, such as 316L stainless steel, to replace it [6-8]. Fabrication of stainless steel helium jackets of SRF cavities necessitates a dissimilar transition joint between niobium and stainless steel. According to standard processing procedures of SRF cavities, this transi-

tion joint is required to maintain high level of hermeticity (leak rate  $< 1 \times 10^{-10}$  mbar · L/s) even after thermal cycle between liquid helium temperature and degassing heat treatment, which can be as high as 873K or 1073K [9]. Therefore, a suitable welding method is required to prepare high strength transition joints.

There is not any successful fusion welding techniques, including electron beam welding, can be applied to join niobium and stainless steel due to the formation intermetallic compounds, mostly between Nb and Fe, in the welded joint [10]. Such brittleness harms the joint strength and may cause vacuum leak after heavy work load [11]. In addition, these compounds cannot withstand heavy thermal load at cryogenic temperatures and eventually fracture occurs. Solid-state welding like diffusion bonding and explosion welding have been developed to joint niobium with stainless steel. Some researchers have used explosive welding to manufacture composite material, such as niobium/stainless steel [12], or titanium/stainless steel/titanium [10,11], to fabricate transition joints. No vacuum leak has been detected on this type of transition joints even after a number of wide-range thermal cycles. High Energy Accelerator Research

<sup>1</sup> CHINESE ACADEMY OF SCIENCES, INSTITUTE OF MODERN PHYSICS, LANZHOU, GANSU 730000, CHINA

<sup>2</sup> THE ADVANCED ENERGY SCIENCE AND TECHNOLOGY GUANGDONG LABORATORY, HUIZHOU, GUANGDONG 516000, CHINA

<sup>3</sup> ANHUI EAST CHINA PHOTOELECTRIC TECHNOLOGY RESEARCH INSTITUTE, WUHU, ANHUI 241002, CHINA

\* Corresponding author: [ttan@impcas.ac.cn](mailto:ttan@impcas.ac.cn)



Organization (KEK) has developed hot isostatic pressing (HIP) to connect niobium/stainless steel and successfully applied it to the SRF cavity [13].

In most of the stainless steel helium jackets, the transition joints between niobium and stainless steel are fabricated by vacuum brazing [14-17]. Moreover, the reliability of brazing joints has been verified by SRF cavities operation experience. Currently, in most laboratories, the most popular filler metal for SRF cavities is oxygen-free copper (OFC). However, recent microstructure analysis revealed that OFC brazed Niobium-stainless steel joint contained a layer of Nb-Fe intermetallic compounds at the Nb/braze interface. These intermetallic compounds can cause brittleness, reduce mechanical properties, and shorten the whole cavity's life. In order to solve this problem, it is necessary to develop new technology to produce no intermetallic compounds, excellent mechanical properties of niobium-stainless steel transition joint.

Kumar et al. thought that there were three approaches to control the diffusion of Fe toward Nb, in which the easiest way to adopt a lower melting point brazing filler metal, thus lower the brazing temperature [18]. The niobium surface suffers from poor wettability as it quickly develops dense oxides when contact with ambient air [19]. Therefore, improving the surface wettability of niobium and reducing the melting point brazing filler metal is a prerequisite for successful brazing the transition joint. Liaw et al. research found that the presence of element Ti was helpful to improve the wettability of niobium surface in the brazing process [20]. Consequently, Kumar et al. had brazed the transition joints with Ag-based active brazing alloy 63Ag-35.25Cu-1.75Ti. The welding temperature of this filler metal was 1123K [18]. It may be noted that nickel plating and addition Ti element were carried out in brazing technique to improve the wettability of niobium. Furthermore, nickel plating can prevent Fe diffusion toward niobium. The results showed that the transition joint without brittle intermetallic layers on any of the two associated interfaces Nb/braze and stainless steel/braze. Nevertheless, compared with OFC filler metal, its mechanical properties were not remarkable enhancement. Guo et al. had reported that silver-copper-palladium (Ag-Cu-Pd) brazing alloy had low vapor pressure, good air tightness, and excellent mechanical properties [21]. Especially, for common base materials (stainless steel, molybdenum and niobium et al.), the filler had excellent wettability. The liquidus of silver-copper-palladium filler metal varies with the content of Pd element (1083K-1223K) [22], and is lower than that of oxygen-free copper (1356K). In the light of above discussions, we believe brazing weld of Nb-stainless steel transition joints with silver-copper-palladium filler metal is a feasible approach.

## 2. Experimental Procedures

In this article, we systematically study the wettability of Ag-Cu-Pd brazing alloys on the niobium, together with the microstructure, mechanical properties, and leak rate of transition joints. Firstly, the wetting angle was measured by the Contact Angle System. Secondly, the morphology and elemental distribution of the welding interface was investigated by scanning electron microscope (SEM) and energy dispersive X-ray spectrometer (EDS), respectively. In the next part, the mechanical properties of the welding samples were characterized by tensile tests and shear tests. Finally, real transition joints were tested with a helium leak detector for leak rates and with a universal testing machine for shear/tensile strengths.

### 2.1. Materials and preparation

In order to fabricate the transition joint at the lowest possible welding temperature, two kinds of filler metal with liquidus of 1123K (Ag-31.5Cu-10Pd) and 1173K (Ag-28Cu-20Pd) were selected, respectively. Two types of base materials were involved in the vacuum brazing, reactor-grade niobium (RRR = 30), 316L type stainless steel. The chemical compositions of niobium and 316L stainless steel were given in TABLE 1, respectively.

Wire-shaped filler metals were studied both in bare samples and transition joints forms. The welding temperature of two kinds of filler metals were 1123-1133K, and 1183K, respectively. The wetting experiment was implemented in accordance with the standards GB/T 11364-2008. The wetting experiment temperature of Ag-31.5Cu-10Pd was 1123K and 1148K, respectively. The wetting experiment temperature of Ag-28Cu-20Pd was 1183K and 1198K, respectively. The holding time of all wettability samples was 10 minutes. The samples were performed in a vacuum furnace at a pressure of with vacuum better than  $5 \times 10^{-4}$  Pa at welding temperature. The welded curve of filler metal was shown in Fig. 1. The welded curve of Ag-31.5Cu-10Pd filler metal was: room temperature-1053K @ 10.1 K/min; soaking at 1053K for 30 min; 1053-1123 @ 7 K/min; soaking at 1123K for 3 min; 1123-893 @ 11.5 K/min; soaking at 893K for 20 min; then naturally cooled to room temperature. The welded curve of Ag-28Cu-20Pd filler metal was: room temperature-1133K @ 10.57 K/min; soaking at 1133K for 30 min; 1133-1183 @ 5 K/min; soaking at 1183K for 4 min; 1183-893 @ 9.6 K/min; soaking at 893K for 20 min; furnace cooling to room temperature. Surface roughness can affect the wettability of filler metal to niobium. Thus, before the brazing, the niobium samples were

TABLE 1

The chemical composition (wt%) of the niobium and 316L stainless steel

Element	Ta	C	Fe	N	W	Mo	Ni	H	Nb
Wt%	0.0762	0.0026	0.0003	0.0006	0.0021	0.001	0.0002	0.0002	Bal
Element	Si	Mn	P	S	Ni	Cr	Mo	C	Fe
Wt%	0.5000	1.370	0.0270	0.0010	10.110	16.650	2.0400	0.0180	Bal

cleaned by two kinds of acid solution. The first way was that niobium was soaked for 20 seconds in a solution of HF, HNO<sub>3</sub>, and H<sub>2</sub>SO<sub>4</sub> (in the ratio of 1:1:2.5). The second way was that niobium was soaked for 4 minutes in a solution of HF, HNO<sub>3</sub>, and H<sub>3</sub>PO<sub>4</sub> (in the ratio of 1:1:2).

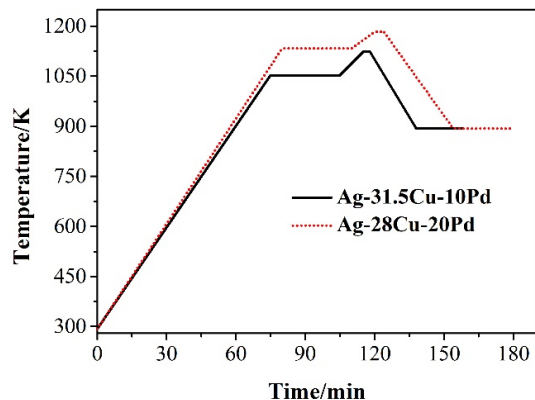


Fig. 1. The welding curve of the filler metal

## 2.2. Sample preparation

The dimensions of niobium and stainless steel samples used to study the wettability of niobium was 40 mm × 40 mm × 3 mm, and study the microstructure of the welding joint was 15 mm

× 15 mm × 3 mm. Filler metal wire of 0.8 mm diameter was placed between the two base materials when welding samples. Filler metal wire of 0.2 g weight was placed on niobium for wetting experiment. The dimension of the transition joint was designed in accordance with the standard GB/Z 25756-2010. After brazing, samples were mechanically polished with sand paper (600, 1000, 2000, 3000 grits), then followed by a standard chemical-mechanical polishing using 0.3 μm alumina slurry.

## 2.3. Mechanics testing

GB standards GB/T 11363-2008 and GB/T 1329-2008 were adopted for testing strength of brazing samples under 300K and 77K (Fig. 2a). The initial shear test samples were prepared in accordance with GB/T 11363-2008. However, the niobium base metal was fracture during the test so that we cannot get the strength of joint. Then, the shear test of samples was implemented in accordance with the standards GB/T 6396-2008 (Fig. 2b). The ultimate shear strength of transition joints was measured with its scheme shown in Fig. 2c. The schematic diagram of the welding of the transition joints was shown in Fig. 2d and Fig. 2e. A plug was inserted in the niobium tube in order to ensure the uniform thickness of transition joints. All tests were completed on a universal testing machine. Schematic diagram of sample shear and transition joint shear shown in Fig. 3.

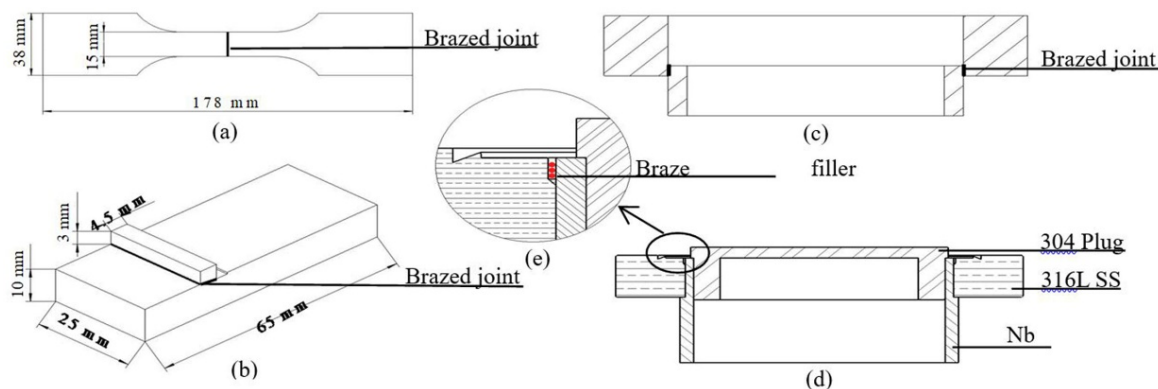


Fig. 2. (a) Dimensional details of tensile test samples (b) Dimensional details of shear test samples (c) Schematic diagram of ultimate shear tests samples (d) Braze joint configuration (e) Partial enlarged view of brazing placement

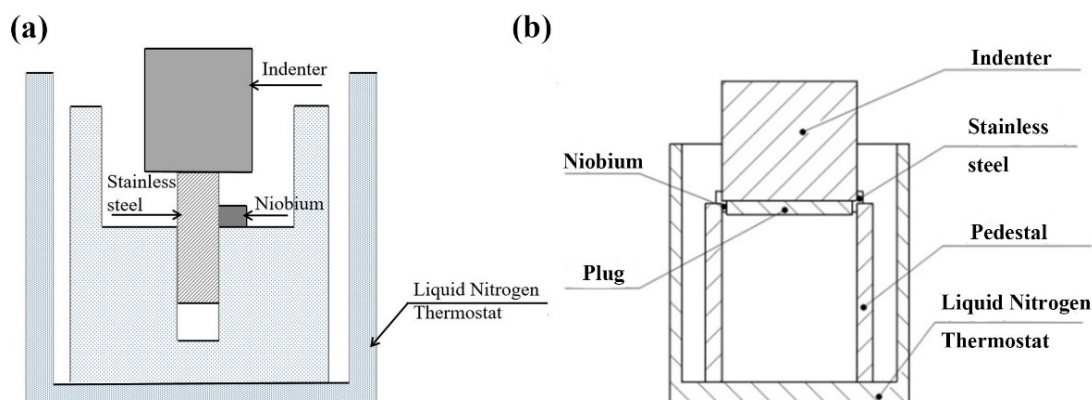


Fig. 3. (a) Schematic diagram of sample shear (b) Schematic diagram of transition joint shear

### 3. Results and discussion

#### 3.1. Wettability of Ag-Cu-Pd filler metals on the niobium

Due to the niobium surface suffers from poor wettability. Firstly, we needed to study the wettability of different Ag-Cu-Pd filler metals on niobium in order to determine which filler metal was selected to prepare the transition joint. In this part, two kinds of acid solutions for cleaning niobium samples were denoted FNS (HF, HNO<sub>3</sub>, and H<sub>2</sub>SO<sub>4</sub>) and FNP (HF, HNO<sub>3</sub>, and H<sub>3</sub>PO<sub>4</sub>).

The spreading area and the contact angle of Ag-Cu-Pd filler metal on niobium surface are shown in Fig. 4 and Fig. 5, respectively, and niobium pieces were cleaned with FNS acid solution before welding. It can be seen that the filler metal wet well on the niobium. The average spreading areas of Ag-31.5Cu-10Pd

were larger than that of Ag-28Cu-20Pd, and the contact angles of Ag-31.5Cu-10Pd were smaller than that of Ag-28Cu-20Pd. These phenomena indicated that the wettability of Ag-31.5Cu-10Pd was better than Ag-28Cu-20Pd. The filler metal diffusion process was initially driven by the surface tension, while the viscous force provided the resistance. Then, the reaction between Pd and Nb would occur and become the dominant force, because Pd and Nb has the trend to be mutually soluble in any proportion. TABLE 2 shows that the contact angles and the spreading areas of Ag-Cu-Pd filler metal under different states on the niobium. The average spreading areas were in the range of 36-143 mm<sup>2</sup>, and the contact angles were in the range of 4°-36°, which indicated good wettability of Ag-Cu-Pd brazing alloys on niobium. It can be found from the TABLE 2 that the spreading area increases with increasing temperature, whereas the wetting angle decreases. The phenomenon implied that the increase of

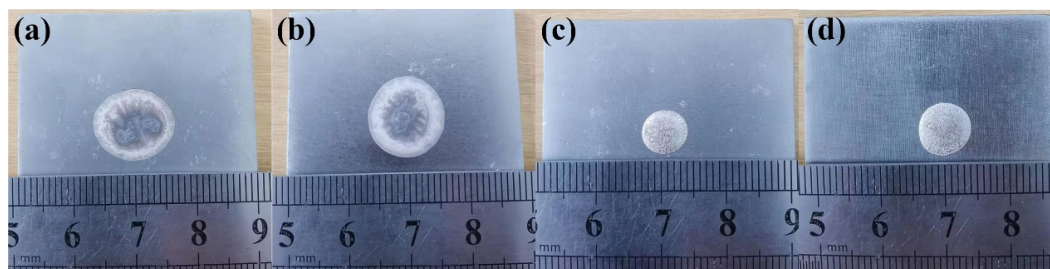


Fig. 4. Surface morphology for spreading of the filler metal (a) Ag-31.5Cu-10Pd at 1123K (b) Ag-31.5Cu-10Pd at 1148K (c) Ag-28Cu-20Pd at 1183K (d) Ag-28Cu-20Pd at 1198K

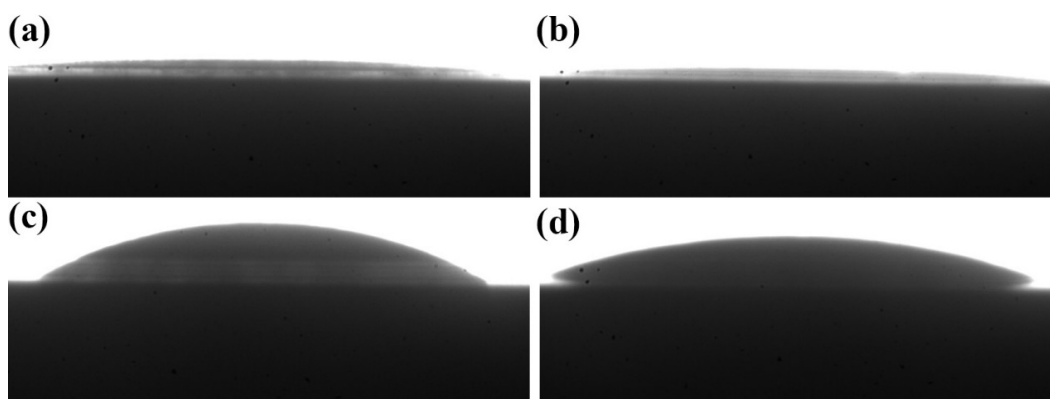


Fig. 5. Figure of wetting angle of the filler metal (a) Ag-31.5Cu-10Pd at 1123K (b) Ag-31.5Cu-10Pd at 1148K (c) Ag-28Cu-20Pd at 1183K (d) Ag-28Cu-20Pd at 1198K

The contact angles and spreading area of Ag-Cu-Pd filler metal

TABLE 2

Filler metal	Cleaning method	Welding temperature (K)	Average contact Angle (°)	Average spreading Area (mm <sup>2</sup> )
Ag31.5-Cu-10Pd	FNS	1133	5.9138	125.8980
Ag31.5-Cu-10Pd	FNP	1133	7.2014	115.6250
Ag31.5-Cu-10Pd	FNS	1148	4.0187	143.8400
Ag31.5-Cu-10Pd	FNP	1148	4.2100	122.1446
Ag-28Cu-20Pd	FNS	1183	28.5889	36.3710
Ag-28Cu-20Pd	FNP	1183	36.5025	36.2176
Ag-28Cu-20Pd	FNS	1198	19.7561	57.8900
Ag-28Cu-20Pd	FNP	1198	26.3160	45.7316

temperature could promote the wetting of the filler metal on the niobium surface. It was also observed that the wettability of the filler metal, which cleaned with FNS acid on the niobium was better than that of FNC acid.

### 3.2. Microstructure of the welded joints

Fig. 6a shows the morphology of the interface of Nb/ Ag-31.5Cu-10Pd /316L stainless steel with brazing temperature of 1123K and holding time of 4 min. A good alloy bond had been formed between the Ag-31.5Cu-10Pd filler metals and the two base materials, and there were no defects such as cracks or pores. The dark gray color zone was the iron (C), the intermediate region was the filler metal layer (D), and the gray color zone was the niobium (E). The intermediate region divided into three sections: the thin diffusion zone near the stainless steel was composed of gray tissue; the thin diffusion was near niobium, consisting mostly of white and a little gray tissue; the remaining area was composed of a large amount of white and a small number of gray strips.

In order to determine the composition of the white and gray regions, we conducted EDS mapping at regions A (gray

phase) and regions B (white phase), and the results were shown in TABLE 3. In region A, the content of Cu was 65.6%, the content of Ag was 12.53%, and the content of Pd was 21.9%, consequently this region was called Cu-rich phase. In region B, the content of Cu was 13.4%, the content of Ag was 80%, consequently the content of Pd is 6.6%, and this region was called Ag-rich phase. As can be seen from the Fe-Ag and Fe-Pd phase diagrams [23], Fe and Pd are easily miscible, while Ag and Fe are immiscible. As a result, Pd tends to diffuse towards Fe, while Ag is far away from Fe, which was consistent with the observation in Fig. 6a, that is, Pd content was high near the Fe/Ag-31.5Cu-10Pd interface (Cu-rich phase). In Fig. 6b, it can be observed that Pd content increases near the interface between the filler metal and the two base metals. This result was consistent with that in Fig. 7. Thus, due to the addition of Pd in the Ag-Cu al-

TABLE 3

The chemical compositions at regions A and regions B in Fig. 6a

Zones	Elemental composition (wt.%)		
	Ag	Cu	Pd
A (gray phase)	12.53	65.6	21.9
B (white phase)	80	13.4	6.6

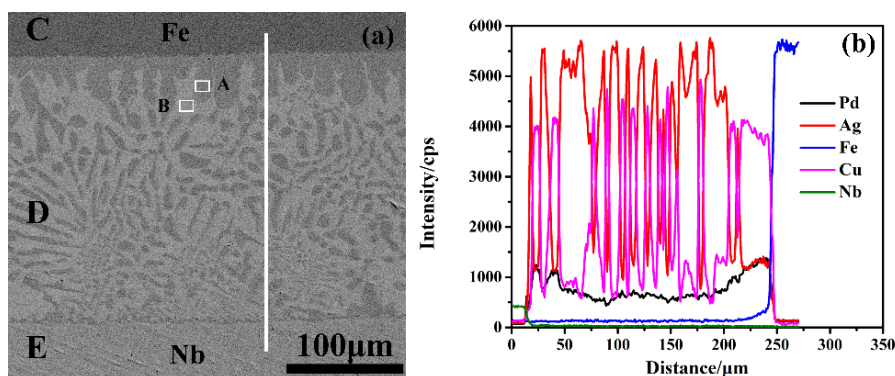


Fig. 6. (a) SEM morphologies of Ag-31.5Cu-10Pd filler metal (b) EDS line scan results across interface marked as straight line in Fig. 6a

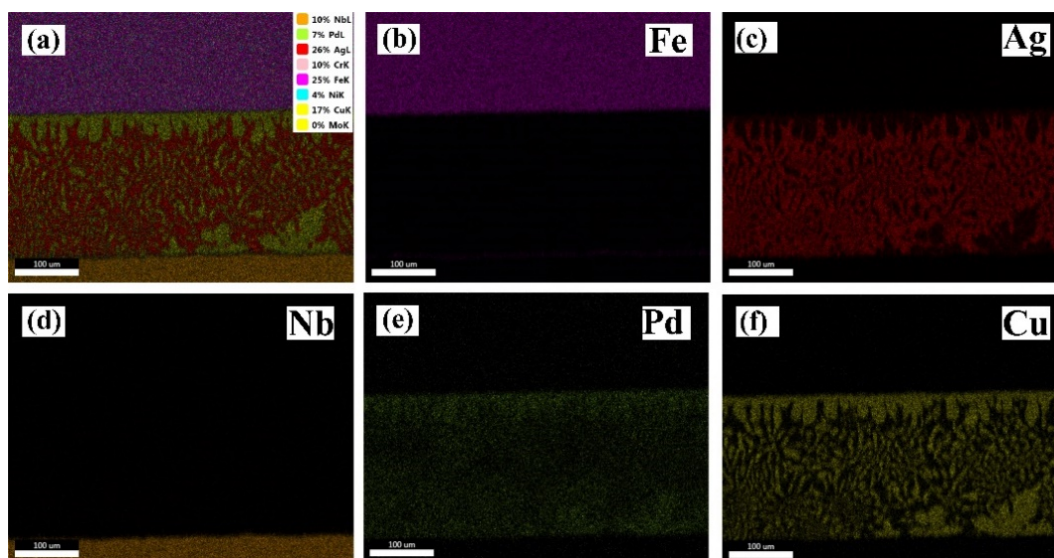


Fig. 7. EDS mapping across the whole brazing surface (Ag-31.5Cu-10Pd filler metal)

loy, the filler metal can be well wet the two base materials and form a good joint.

Fig. 8a shows the morphology of the interface of Nb/Ag-28Cu-20Pd /316L stainless steel with brazing temperature of 1183K and holding time of 4 min. A great alloy bond had been formed between the Ag-28Cu-20Pd filler metals and the two parent materials, and there were no defects such as cracks and pores. The dark color zone was the iron (C), the intermediate region was the filler metal layer (D), and the gray color zone was the niobium (E). The intermediate region divided into three sections: the thin diffusion zone near the stainless steel was composed of large gray tissue; the thin diffusion was near niobium, consisting mostly of white tissue; the remaining area was composed of a large amount of white and a part of large gray tissue.

TABLE 4

The chemical compositions at regions A and regions B in Fig. 8a

Zones	Element composition (wt.%)		
	Ag	Cu	Pd
A (white phase)	73.1	21.9	5
B (gray phase)	12.5	68.1	19.4

In order to determine the composition of the white and grey regions, we conducted EDS mapping at regions at regions A (white phase) and regions B (gray phase), and the results were shown in TABLE 4. In region A, the content of Cu was 21.9%, the content of Ag was 73.1%, and the content of Pd was 5%, and this region was called Ag-rich phase. In region B, the content of Cu was 68.1%, the content of Ag was 12.5%, and the content of Pd was 19.4%, and this region was called Cu-rich phase. It also can be seen from Fig. 6a and Fig. 8a that the gray regions and the white regions in Ag-28Cu-20Pd filler metal were significantly coarser than that in Ag-31.5Cu-10Pd filler metal. Therefore, it can be considered that the coarsening of Cu-rich phase and the coarsening of Ag-rich phase not only leads to poor spreading property but also reduce the mechanical properties of the joint. In Fig. 8b, it can be observed that Pd content increases near the interface between the filler metal and the two base metals. Moreover, Pd element distribution was more uniform than that in Fig. 6b at the welding surface. This phenomenon shows that the high Pd content was beneficial to the mutual diffusion between the filler metal and the base metal at the interfaces.

In order to verified whether intermetallic compounds were formed in the welding process, EDS line scan was performed on

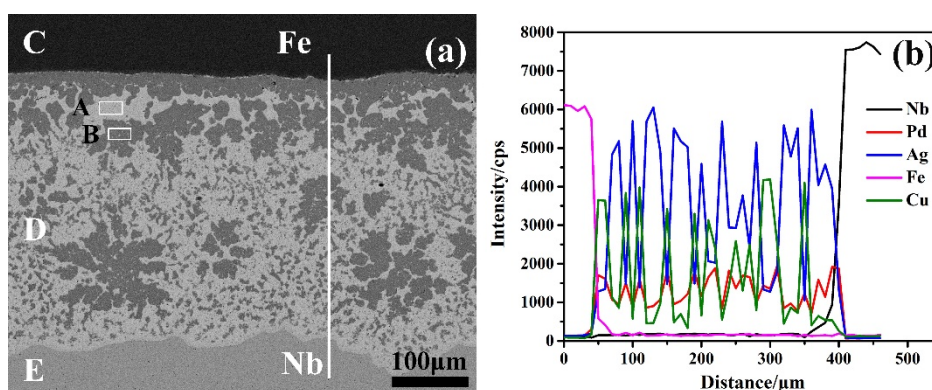


Fig. 8. (a) SEM morphologies of Ag-28Cu-20Pd filler metal (b) EDS line scan results across interface marked as straight line in Fig. 8

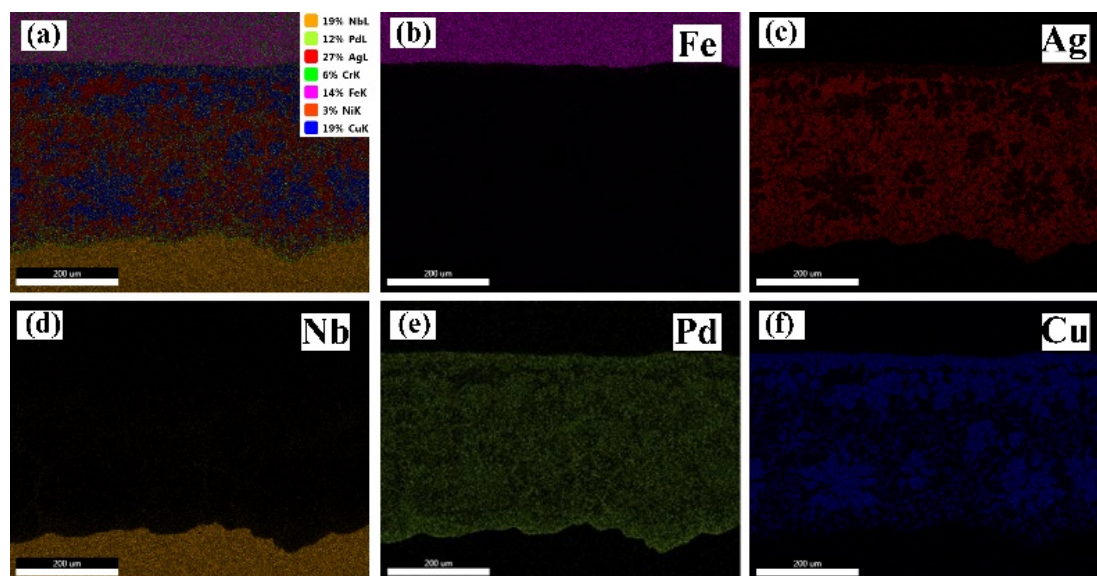


Fig. 9. EDS mapping across the whole brazing surface (Ag-28Cu-20Pd filler metal)

the bonding surface of the sample. The scan path was shown by the straight line in Fig. 6b and Fig. 8b. It can be seen from Fig. 6b and Fig. 8b that Fe element was not observed at the bonding surface of Nb/AgCuPd with either kind of filler metals. Thus, there's no need to worry about Fe-Nb intermetallic compounds in this region. It was also found that the elemental composition shifted away from stoichiometry near the two interfaces, indicating moderate level of mutual diffusion between base and filler metals. All the above appearance was necessary for forming joints with good performance. Fig. 7 and Fig. 9 were EDS mapping of the bonding interface of the two kinds of joints, and it can be evidently observed that there was no Fe element in the Nb/AgCuPd bonding surface.

### 3.3. Brazing joint strength

In order to verify that the presence of intermetallic compounds could reduce the mechanical properties of the transition joint, the mechanical properties of the samples were investigated. TABLE 5 shows that the average tensile strength and the average shear strength of the welded joint under different filler metal, different ambient temperature. The tensile strength and shear strength test was adopted three samples in one state.

TABLE 5

The tensile strength and shear of sample

Filler metal	Test temperature (K)	Average tensile strength (MPa)	Average shear Strength (MPa)
Ag-31.5Cu-10Pd	300	167.3	178.2
Ag-31.5Cu-10Pd	77	394	349
Ag-28Cu-20Pd	300	110.5	149
Ag-28Cu-20Pd	77	124	142

It can be seen from the TABLE 5 that the tensile strength of the samples prepared with Ag-31.5Cu-10Pd filler metal at 300K were lower than that at 77K, and the tensile strength at 77K was 2.3 times of that at 300K. The tensile strength of Ag-31.5Cu-10Pd filler metal at 300K was higher than that of 63Ag-35.25Cu-1.75Ti filler metal (122 ~ 143 MPa) [18] and oxygen-free copper filler metal (76 ~ 96 MPa) [24]. The microstructure shows that no intermetallic chemicals were formed in the samples prepared with Ag-31.5Cu-10Pd and 63Ag-35.25Cu-1.7 filler metal, which indicated that intermetallic compounds could indeed reduce the mechanical properties of the transition joints. The tensile strength of the sample prepared by Ag-28Cu-20Pd filler metal was slightly higher than that of the oxygen-free filler metal at 300K. Due to the poor wettability between filler metal and niobium and the coarsening of Cu-rich phase and the coarsening of Ag-rich phase during welding, then, the tensile strength of the sample was low.

At 300K, shear testing of the samples prepared with Ag-31.5Cu-10Pd filler metal exhibited shear strength in the range of 170-183 MPa, and larger than the samples prepared with 63Ag-35.25Cu-1.75Ti filler metal in literature (80-133

MPa) [18]. The shear strength of the samples prepared by Ag-31.5Cu-10Pd filler metal at 77K was twice that at 300K. At 300K, the average shear strength of the samples prepared with Ag-28Cu-20Pd filler metal was little different from that of 77K, and the degradation of shear strength did not appear at 77K. It can be seen from the above results that Ag-31.5Cu-10Pd filler metal can well wetting niobium and there was no formation of intermetallic brittle compounds in the welding process. Whereas it has the best mechanical properties in the existing literature. In the welding process of Ag-28Cu-20Pd filler metal, the coarsening of Cu-rich phase and Ag-rich phase, the poor performance of its wetting niobium resulted in its mechanical properties not reaching the expected level.

There were two reasons of the mechanical properties of the samples prepared by Ag-31.5Cu-10Pd filler metal at 77K were better than those at 300K. The first reason was that the mechanical properties of the base metal and filler metal increase at 77K. The second reason was that low temperature soaking makes the weld microstructure fine. Due to the presence of the coarsening of Cu-rich phase and Ag-rich phase in the weld, which leads to insufficient refinement of the microstructure after low temperature immersion. Therefore, it can be considered that the mechanical properties of the samples prepared by Ag-28Cu-20Pd filler metal were not significantly improved at 77K.

### 3.4. Welding and leak detection of transition joints

Due to the excellent mechanical properties of the sample was prepared by Ag-31.5Cu-10Pd filler metal. Thus, in this part, the transition joints would be prepared by Ag-31.5Cu-10Pd brazing filler metal, and vacuum leak detection was carried out. The thermal expansion coefficient of stainless steel is close to 2.6 times larger than that of niobium at the brazing temperature, which brings challenges to the uniform thickness of the weld. Therefore, during the welding process, the requirement weld thickness at brazing temperature was ensured by inserting a stainless steel plug into niobium pipe. The same technique also adopted by many laboratories to maintain the desired gap between niobium and stainless steel tubular parts during brazing [18]. The stainless steel plug was machined out after brazing. Before the helium leak test, in order to simulate the cavity heat treatment process, the transition joints had been heat treatment at 873K for 2 h in vacuum furnace.

In this paper, we had been selected three types of transition joints which defined as CF80 (niobium tube inner diameter 80 mm), CF100 (niobium tube inner diameter 94 mm) and CF150 (niobium tube inner diameter 105 mm), respectively. The vacuum leak detection was adopted three transition joints in one type. Fig. 10 shows the transition joint prepared with Ag-31.5Cu-10Pd filler metal. It can be seen from the Fig. 10a that there were pores and some black defects between niobium and stainless steel. The pores indicate that the filler metal was not fully flowing, and the black defects indicate that the filler metal was not fully melted. It can be seen from Fig. 10b that

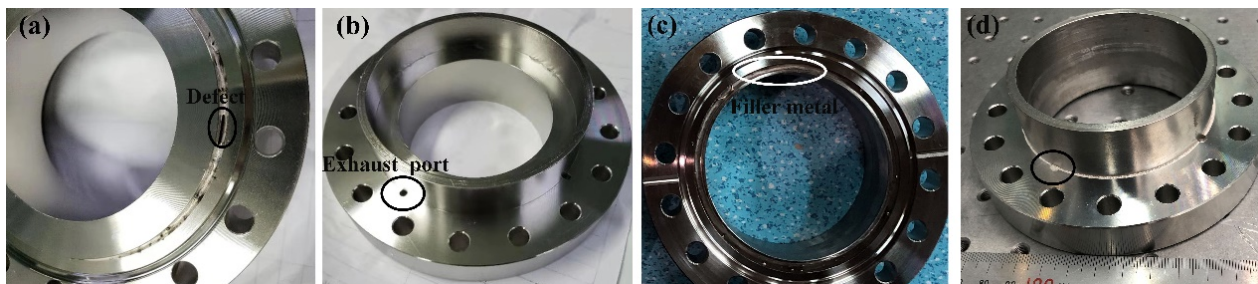


Fig. 10. Picture of transition joint

there was no filler metal in the hole on the back of the transition joint. This result indicated that the filler metal did not fill the gap between niobium and stainless steel at the welding temperature of 1123K. The function of the hole was to make the gas in the gap between niobium and stainless steel easy to discharge during welding. It also can be observed from Fig. 10b that there was no filler metal in the contact position between stainless steel and niobium. Finally, the transition joints were cleaned by ultrasonic, and vacuum leak detection. The result showed that the transition joint had vacuum leakage. Therefore, it was not feasible to weld the transition joint with the technology of welding sample. The reason was that the solder was easy to flow due to the small welding area and uniform heating of the sample. Moreover, the large welding area of the transition joint and the nonuniform heating of the transition joint result in the solder could not be fully non-melting at the welding temperature of 1123K. Fig. 10c shows the transition joint prepared at the welding temperature of 1133K and the holding time of 4 min. It can be seen from the figure that there were no pores and black defects. It can also be seen from Fig. 10d that the hole on the back was completely filled with filler metal and the contact surface of niobium and stainless steel had filler metal overflow. The vacuum leak detection result shows that no vacuum leakage occurs in the transition joint.

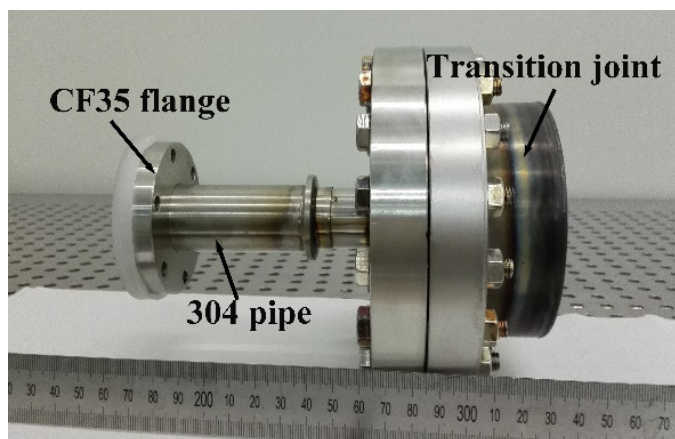


Fig. 11. Assembly used for vacuum leak tests

Fig. 11 shows the transition joint standby for leak detection after assembly. The assembly used for helium leak testing composed of a 304 stainless steel knife edge flange for connecting

the transition joint, a certain length adapter pipe of 304 stainless steel and a DN35 stainless steel knife edge flange for connecting the metal bellows. The other side of standard metal bellows was connected to the helium leak detector through a standard stainless steel bellows. The niobium tube away from the flange side was welding with the 3 mm niobium plate by argon arc welding. It should be noted that stainless steel flanges were sealed with OFE copper gasket. After withstanding ten cryogenic shocks with liquid nitrogen, the joints still show leakage rate below  $1.1 \times 10^{-11}$  mbar · L/s both at room temperature and liquid nitrogen temperature. It should be noted that most of the contraction of materials occur between 300 and 77 K [18]. Hence, the thermal cycling test between 300 and 77 K (in place of 4 K) should give preliminary validation of reliability of the transition joints against service-induced low cycle fatigue conditions.

### 3.5. Ultimate shear strength

TABLE 6 shows the average shear strength of different types of transition joints. Each type was tested three times. It can be seen from TABLE 6 that the average shear strength is 357 MPa at 300K and 439 MPa at 77K, and, it was better than the transition joint prepared with oxygen free copper filler metal in the literature. It is also found from TABLE 6 that the consistency of the three types of transition joints was good, indicating good feasibility to prepare transition joints with Ag-Cu-Pd as brazing fillers. In addition, the shear strengths of the transition joints were greater than the samples. The difference was more obvious at 77K, and such enhancement results from the strictly controlled thickness of the weld joint.

TABLE 6

The shear strength of transition joint

Filler metal	Type of transition joint	Test temperature (K)	Average shear Strength (MPa)
Ag-31.5Cu-10Pd	CF80	300	356
Ag-31.5Cu-10Pd	CF80	77	440
Ag-31.5Cu-10Pd	CF100	300	362
Ag-31.5Cu-10Pd	CF100	77	446
Ag-31.5Cu-10Pd	CF150	300	375
Ag-31.5Cu-10Pd	CF150	77	457



#### 4. Conclusion

In our work, niobium-316L stainless steel transition joints were prepared successfully by vacuum brazing method. The wettability of Ag-Cu-Pd filler metals on the niobium, the interface microstructure and mechanical properties of the transition joints were investigated. The conclusions can be summarized as follows:

- 1) The wettability of different Ag-Cu-Pd filler metals on niobium were investigated. Two kinds of filler metals had been wet well on the niobium. The spreading area of Ag-31.5Cu-10Pd filler metal was larger than that of Ag-28Cu-20Pd filler metal, and contact angle of Ag-31.5Cu-10Pd filler metal was less than that of Ag-28Cu-20Pd filler metal. Therefore, the Ag-31.5Cu-10Pd filler metal wettability on niobium better than Ag-28Cu-20Pd filler metal. The wettability of the filler metal cleaned with FNS acid on the niobium was better than that of FNC acid.
- 2) Microstructure was observed on both sides of the welding seam of two kinds of filler metals while no visible defects such as cracks and pores were seen. The microstructure distribution of Ag-31.5Cu-10Pd filler metal was relatively uniform, while the coarsening of Cu-rich phase and Ag-rich phase occurs in Ag-28Cu-20Pd filler metal. The EDS line scan and mapping results revealed that the no presence of Fe at the Nb/Cu interface leads to not formation of intermetallic compounds.
- 3) Owing to Ag-31.5Cu-10Pd filler metal can be well wet niobium, and there was no formation of intermetallic brittle compounds in the welding process. Therefore, it had the best mechanical properties both room temperature (300K) and liquid nitrogen temperature (77K) at present. In the welding process of Ag-28Cu-20Pd filler metal, due to the coarsening of Cu as well as the poor performance of its wetting niobium led to its mechanical properties not reaching the expected level.
- 4) According to the brazing experience of samples, different types of transition joints can be successfully prepared. After 10 cold shocks of liquid nitrogen, the leak rates are better than  $1.1 \times 10^{-9}$  mbar · L/s. During the brazing process, the thickness of the weld was strictly controlled in order to obtain transition joints with good strengths. In the future, we will try to fabricate the transition joint on the SRF cavities.

#### Acknowledgements

The present work was supported by National Natural Science Foundation of China (Grant No. 12075295).

#### Compliance with Ethical Standards

Conflict of Interest: The authors declare that they have no conflict of interests

#### REFERENCES

- [1] W.L. Zhan, Accelerator Driven Sustainable Fission Energy, in: Proceedings of 7th International Particle Accelerator Conference, Busan, Korea, 4271-4275 (2016).  
<https://epaper.kek.jp/ipac2016/papers/frvaa03.pdf>
- [2] G.Q. Xiao, H.S. Xu, S.C. Wang, HIAF and CiADS national research facilities: Progress and prospect, Nucl. Phys. Rev. **34**, 275-283 (2017).  
DOI: <https://doi.org/10.11804/NuclPhysRev.34.03.275>
- [3] S.H. Liu, Z.J. Wang, Y. Tao, Y. He, H. Jia, Z.P. Xie, W.P. Dou, W.L. Chen, W.S. Wang, Y.Z. Jia, C. Wang, Physics design of the superconducting section of the CiADS linac, Int. J. Mod. Phys. A **34**, 1950178 (2019).  
DOI: <https://doi.org/10.1142/S0217751X19501781>
- [4] W.M. Yue, S.X. Zhang, C.L. Li, T.C. Jiang, L.B. Liu, R.X. Wang, Y.L. Huang, T. Tan, H. Guo, E. Zaplatin, P.R. Xiong, A.D. Wu, F.F. Wang, S.H. Zhang, S.C. Huang, Y. He, Z.E. Yao, H.W. Zhao, Design, fabrication and test of a taper-type half-wave superconducting cavity with the optimal beta of 0.15 at Imp, Nucl. Eng. Technol. **52**, 1777-1783 (2020).  
DOI: <https://doi.org/10.1016/j.net.2020.01.014>
- [5] E.A. Brandes, G.B. Brook, Smithells Metals Reference Book, 7th edn, Butterworth-Heinemann Oxford, 14.3-14.5 (2000).
- [6] H. Kaiser, G. Meyer, H.B. Peters, G. Weichert, Helium Vessel for the TTF Cavity, TESLA Collaboration Report 94-26, 1994.
- [7] C. Grimm, T. Arkan, M. Foley, T. Khabiboulline, D. Watkins, 1.3 GHz RF Nb Cavity to Ti Helium Vessel TIG Welding Process at Fermi Lab, in: 14th International Conference on RF Superconductivity, Berlin, German, 669-671 (2009).  
<https://accelconf.web.cern.ch/srf2009/papers/thppo041.pdf>
- [8] H. Saignac, S. Rousselot, C. Commeaux, H. Gassot, T. Junquera, P. Bosland, H. Safa, Preliminary Design of Stainless Steel Helium Tank and its Associated Cold Tuning System for 700 MHz SCRF Cavities for Proton, in: Proceedings of the 10th Workshop on RF Superconductivity, Tsukuba, Japan, 540-542 (2001).  
<https://accelconf.web.cern.ch/srf01/papers/pt022.pdf>
- [9] Y. Xie, Development of Superconducting RF Sample Host Cavities and Study of Pit-induced Cavity Quench, PhD thesis, Cornell University, (2013).
- [10] B. Sabirov, J. Budagov, G. Shirkov, Y. Taran, Recent optimized design of ilc cryomodule with explosion welding technology, in: XXV Russian Particle Accelerator Conference, Petersburg, Russia, 141-143 (2016).  
<https://accelconf.web.cern.ch/rupac2016/papers/thcdmh02.pdf>
- [11] B.M. Sabirov, J.A. Budagov, G.D. Shirkov, First samples of Ti and Nb tubes explosion welding joint with stainless steel for ILC 1.8 K cryomodule, Phys. Part. Nuclei **44**, 728-756 (2013).  
DOI: <https://doi.org/10.1134/S1063779613040059>
- [12] R.X. Wang, Y. He, T. Tan, X.P. Guo, J. Song, J.S. Ren, S.H. Zhang, X.Y. Zhang, Niobium-316L Stainless Steel Transition Joints for Superconducting Radiofrequency Cavities by Explosive Welding, Rare Metal. Mat. Eng. **48**, 3876-3882 (2019).  
[http://www.rmme.ac.cn/rmme/ch/reader/view\\_abstract.aspx?file\\_no=20181123&flag=1](http://www.rmme.ac.cn/rmme/ch/reader/view_abstract.aspx?file_no=20181123&flag=1)

- [13] K. Saito, H. Inoue, H. Ao, N. Satoh, Stainless flange bonded to niobium tube and simple aluminum sealing, in: Proceedings of the 10th Workshop on RF Superconductivity, Tsukuba, Japan, 531-534 (2001). <https://accelconf.web.cern.ch/srf01/papers/pt020.pdf>
- [14] J.D. Fuerst, W.F. Toter, K.W. Shepared, Niobium to stainless steel braze transition development, in: 11th Workshop on RF Superconductivity, Lubeck, German 305-307 (2003). <https://accelconf.web.cern.ch/SRF2003/papers/tup11.pdf>
- [15] E.C. Reece, E.F. Daly, J. Henry, W.R. Hicks, J. Preble, H. Wang, G. Wu, Optimization of the srf cavity design for the cefab 12gev upgrade, in: 13th International Workshop on RF Superconductivity, Beijing, China, 536-539 (2007). <https://accelconf.web.cern.ch/srf2007/PAPERS/WEP31.pdf>
- [16] L. Ristori, W. Toter, Development at anl of a copper-brazed joint for the coupling of the niobium cavity end wall to the stainless steel helium vessel in the fermilab ssr1 resonator, in: International Particle Accelerator Conference 2012, New Orleans, USA, 2345-2347 (2012). <https://accelconf.web.cern.ch/IPAC2012/papers/weppc058.pdf>
- [17] O. Capatina, S. Atieh, I. Aviles Santillana, G. Arnau Izquierdo, R. Bonomi, S. Calatroni, J. Chambrillon, F. Gerigk, R. Garoby, M. Guinchard, T. Junginger, M. Malabaila, L. Marques Antunes Ferreira, S. Mikulas, V. Parma, F. Pillon, T. Renaglia, K. Schirm, T. Tardy, M. Therasse, A. Vacca, N. Valverde Alonso, A. Vande Craen, Cern developments for 704 mhz superconducting cavities, in: Proceedings of the 16th International Conference on RF Superconductivity, Paris, France, 1198-1211 (2013). <https://accelconf.web.cern.ch/SRF2013/papers/frlob04.pdf>
- [18] A. Kumar, P. Ganesh, R. Kaul, V.K. Bhatnagar, K. Yedle, P. Ram Sankar, A New Vacuum Brazing Route for Niobium-316L Stainless Steel Transition Joints for Superconducting RF Cavities, *J. Mater. Eng. Perform.* **24**, 952-963 (2015). DOI: <https://doi.org/10.1007/s11665-014-1312-1>
- [19] A.J. Palmer, C.J. Woolstenhulme, Brazing Refractory Metals used in High-temperature Nuclear Instrumentation, in: International Conference on Advancements in Nuclear Instrumentation Measurement Methods and their Applications, Marseille, France, 1-5 (2009). <https://www.osti.gov/servlets/purl/961932>
- [20] D.W. Liaw, R.K. Shiue, Brazing of Ti-6Al-4V and Niobium Using Three Silver-Base Braze Alloys, *Metal. Mater. Trans. A* **36**, 2415-2427 (2005). DOI: <https://doi.org/10.1007/s11661-005-0114-3>
- [21] F.F. Guo, X.Y. Chen, X.M. Shi, Y.F. Qi, G.Q. Zhang, X.M. Huang, Y. Qi, Effect of Pd content on microstructure and properties of Ag-Cu-Pd solder, *Nonferr. Met. Sci. Eng.* **8**, 64-68 (2017). DOI: <https://doi.org/10.13264/j.cnki.ysjksx.2017.03.010>
- [22] Y.E. Li, T. Jiang, X.L. Sun, G. Ma, Brazing material used for common metal materials in vacuum electron devices, *Hot Working Technology* **39**, 203-205 (2010). DOI: <https://doi.org/10.14158/j.cnki.1001-3814.2010.23.061>
- [23] S. Nagasaki, M. Hirabayashi, Binary Alloy Phase-diagrams, first edn, AGNE Gijutsu Center Co, Ltd, Tokyo, 35-36, 2002.
- [24] R.X. Wang, Y.L. Huang, T.C. Jiang, H. Guo, P.R. Xiong, T. Tan, W.M. Yue, Z.L. Zhang, Y. He, X.Y. Zhang, Microstructure and Mechanical Properties of Niobium and 316 L Stainless Steel Joints by TU1 Oxygen Free Copper Brazing, *Rare Metal Materials and Engineering*, *Rare Metal. Mat. Eng.* **50**, 1166-1172 (2021). [http://www.rmme.ac.cn/rmme/ch/reader/view\\_abstract.aspx?file\\_no=20200220&flag=1](http://www.rmme.ac.cn/rmme/ch/reader/view_abstract.aspx?file_no=20200220&flag=1)